Zygmunt PIATEK[1], Bernard BARON[2], Paweł JABŁOŃSKI[1], Tomasz SZCZEGIELNIAK[1], Dariusz KUSIAK[1], Artur PASIERBEK[3]

Czestochowa University of Technology (1), Opole University of Technology (2), The Silesian University of Technology (3)

doi:10.15199/48.2015.12.50

A numerical-analytical method for magnetic field determination in three-phase busbars of rectangular cross section

Abstract. *A numerical-analytical method for determining the magnetic field distributions in high-current busducts of rectangular busbars is presented in this paper. The approach is based on the Partial Element Equivalent Circuit (PEEC) method. The integral equations are solved numerically to determine the current density distribution throughout the busbars. Then the values are used in analytical formulas to find the magnetic field around the busbars. The method takes into account the skin effect and proximity effects, as well as the complete electromagnetic coupling between phase bars and the neutral bar. Two applications to three-phase unshielded systems of busbars are presented.*

Streszczenie. *W artykule przedstawiono numeryczno-analityczną metodę obliczania pola magnetycznego układów szyn prostokątnych. Metoda oparta jest na teorii obwodowych cząstkowych elementów zastępczych. Najpierw rozwiązywane są numerycznie równania całkowe dla gęstości prądu w szynach. Następnie otrzymane wartości są wykorzystane w analitycznych wzorach na pole magnetyczne wokół szyn. Metoda uwzględnia zjawisko naskórkowości i zbliżenia oraz całkowite sprzężenie magnetyczne miedzy szynoprzewodami. Przedstawiono wyniki obliczeniowe dla dwóch układów nieekranowanych trójfazowych szynoprzewodów prostokątnych. (**Numeryczno-analityczna metoda obliczania pola magnetycznego układu szynoprzewodów prostokątnych**)*

Keywords: Rectangular busbar, high-current bus duct, magnetic field, numerical-analytical method.
Słowa kluczowe: Prostokątny przewód szynowy, tor wielkoprądowy, pole magnetyczne, metoda numeryczno-analityczna.

Introduction

High-current air-insulated bus duct systems with rectangular busbars are often used in power generation and substation, due to their easy installation and utilization. The increasing power level of these plants requires an increase in the current-carrying capacity of the distribution lines (usually 1-10 kA). The medium voltage level of the generator terminals is 10-30 kV. The construction of busbar is usually carried out by putting together several flat rectangular bars in parallel for each phase in order to reduce thermal stresses. The spacing between the bars is made equal to their thickness for practical reasons, and this leads to skin and proximity effects. The bus ducts usually consist of aluminum or copper busbars [1, 2]. A typical cross-section of the unshielded three-phase high-current bus duct is depicted in Fig. 1.

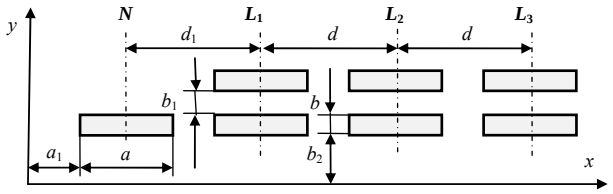

Fig. 1. Three phase high-current bus duct of rectangular cross-section with two busbars per phase and one neutral busbar

Power busbars generate extremely low frequency magnetic field, which can cause disturbances nearby computers and some other electrical, electronic and digital devices. Power distribution three-phase busbar systems belong to the main sources of magnetic field of industrial frequency, and can generate electromagnetic interference by inductive coupling. Moreover, the presence of a low frequency magnetic field generated by power busbars may produce some undesirable effects on human health [3-6]. Thus, a correct prediction of the magnetic field generated by high current bus ducts is very important.

The distribution of AC magnetic field in the region surrounding the busbars can be found exactly for simple geometries, only, like round wires and tubes [7], or very long and thin rectangular busbars (tapes or strips) [8-10]. For more complex cross-sections analytical-numerical and numerical methods must be used to find the magnetic field distributions, which is further modified by the proximity of other conductors – "proximity effect" [4-6, 11-15]. Both the skin effect and proximity effect will generally cause the magnetic field distribution differs considerably from the expected one without taking into account both effects. The development of efficient numerical or analytical methods for the solutions of these problems is therefore of interest.

Multiconductor model of the busbars

In this model, each phase, neutral busbars and each plate of enclosure is divided in several thin subbars [2, 26-31], as shown in Fig. 2.

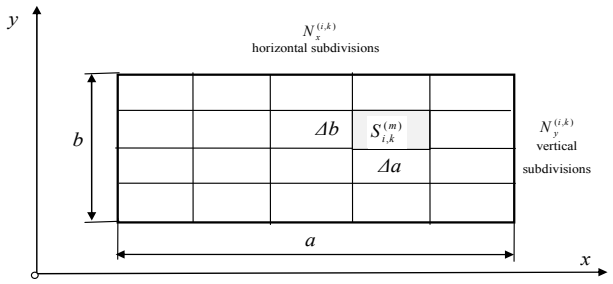

Fig. 2. The k^{th} bar of the i^{th} phase divided into $N_{i,k} = N_x^{(i,k)} N_y^{(i,k)}$ subbars

This division of the k^{th} bar of the i^{th} phase or the neutral into subbars is carried out separately for the horizontal (Ox axis) and vertical (Oy axis) direction of its cross-sectional area. Hence, the subbars are generally rectangular in their cross-section, with the width Δa and thickness Δb, defined by the following relations:

$$\Delta a = \frac{a}{N_x^{(i,k)}} \quad \text{and} \quad \Delta b = \frac{b}{N_y^{(i,k)}}, \tag{1}$$

where a and b are the width and the thickness of the busbar, respectively, $N_x^{(i,k)}$ and $N_y^{(i,k)}$ are the number of divisions along the busbar width and thickness respectively. Thus, the total number of subbars of the k^{th} bar of the i^{th}

phase is $N_{i,k} = N_x^{(i,k)} N_y^{(i,k)}$, and they are numbered by m = 1, 2, …, $N_{i,k}$. For the l^{th} bar of the j^{th} phase or the neutral we have the total number of subbars $N_{j,l} = N_x^{(j,l)} N_y^{(j,l)}$ numbered by n = 1, 2, …, $N_{j,l}$. All subbars have the same length l.

If the area $S_{i,k}^{(m)} = \Delta a \cdot \Delta b$ of the m^{th} subbar is very small and the diagonal $[(\Delta a)^2+(\Delta b)^2]^{1/2}$ of it is not greater than skin depth, we can neglect the skin effect and assume that the complex current density can be considered uniform throughout the subbar, i.e.

$$\underline{J}_{i,k}^{(m)} = \frac{\underline{I}_{i,k}^{(m)}}{S_{i,k}^{(m)}} \tag{2}$$

where $\underline{I}_{i,k}^{(m)}$ is the complex current flowing through the m^{th} subbar.

Current densities

For the m^{th} subbar the integral equation can be written as follows [16]

$$\frac{\underline{J}_{i,k}^{(m)}(X)}{\sigma_i} + \frac{\mathrm{j}\omega\mu_0}{4\pi} \sum_{j=1}^{N_c} \sum_{l=1}^{N_j} \sum_{n=1}^{N_{j,l}} \int_{v_{t,l}} \frac{\underline{J}_{j,l}^{(n)}(Y)}{\rho_{XY}} \mathrm{d}v_{j,l}^{(n)} = \underline{u}_i \tag{3}$$

where $v_{j,l}^{(n)}$ is the volume of the n^{th} subbar or plate of the l^{th} bar or plate of the j^{th} phase or the neutral or the enclosure, and $\rho_{XY} = |X - Y|$ is the distance between the observation point $X = (x_1, y_1, z_1)$ and the source point $Y = (x_2, y_2, z_2)$.

Now, we can divide Eq. (3) by the area $S_{i,k}^{(m)}$ and integrate over the volume $v_{i,k}^{(m)}$ of the m^{th} subbar or plate, obtaining the following equation:

$$R_{i,k}^{(m)} \underline{I}_{i,k}^{(m)} + \mathrm{j}\omega \sum_{j=1}^{N_c} \sum_{l=1}^{N_j} \sum_{n=1}^{N_{j,l}} M_{(i,k)(j,l)}^{(m,n)} \underline{I}_{j,l}^{(n)} = \underline{U}_i \,, \tag{4}$$

where $\underline{U}_i$ is the voltage drop across of all subbars of the i^{th} phase or the neutral or the shield (they are connected in parallel), and the resistance of the m^{th} subbar is defined by

$$R_{i,k}^{(m)} = \frac{l}{\sigma_i S_{i,k}^{(m)}} \,, \tag{5}$$

and the self or the mutual inductance is expressed as

$$M_{(i,k)(j,l)}^{(m,n)} = \frac{\mu_0}{4\pi\, S_{i,k}^{(m)} S_{j,l}^{(n)}} \int_{v_{i,k}^{(m)}} \int_{v_{j,l}^{(n)}} \frac{\mathrm{d}v_{i,k}^{(m)}\, \mathrm{d}v_{j,l}^{(n)}}{\rho_{XY}} \,. \tag{6}$$

The exact closed formulae for the self and the mutual inductance of rectangular conductor of any dimensions, including any length, are given in [18] and [19] respectively. Not only do not we use the geometric mean distance here, we do not use the formula for mutual inductance between two filament wires as well.

The set of equations like as (4), written for all subbars, forms the following general system of complex linear algebraic equations

$$\hat{\underline{U}} = \hat{\underline{\boldsymbol{Z}}}\, \hat{\underline{\boldsymbol{I}}} \,, \tag{7}$$

where $\hat{\underline{U}}$ and $\hat{\underline{I}}$ are column vectors of the voltages and currents of all subbars, respectively, and $\hat{\underline{\boldsymbol{Z}}}$ is the symmetric matrix of self and mutual impedances (the impedance matrix) of all subbars, the elements of which are

$$\underline{Z}_{(i,k)(j,l)}^{(m,n)} = \begin{cases} R_{i,k}^{(m)} + \mathrm{j}\omega\, M_{(i,k)(j,l)}^{(m,n)} & m = n, i = j, k = l, \\ \mathrm{j}\omega\, M_{(i,k)(j,l)}^{(m,n)} & \text{otherwise.} \end{cases} \tag{8}$$

Then, we can find the admittance matrix $\hat{\underline{\boldsymbol{Y}}}$, which is the inverse matrix of the impedance matrix $\hat{\underline{\boldsymbol{Z}}}$, and it is expressed as

$$\hat{\underline{\boldsymbol{Y}}} = \left[\underline{Y}_{(i,k)(j,l)}^{(m,n)}\right] = \hat{\underline{\boldsymbol{Z}}}^{-1} \,, \tag{9}$$

and has a similar structure as $\hat{\underline{\boldsymbol{Z}}}$. Then it is possible to determine the current of the m^{th} subbar of the k^{th} bar of the i^{th} phase or the neutral as

$$\underline{I}_{i,k}^{(m)} = \sum_{j=1}^{N_c} \sum_{l=1}^{N_j} \sum_{n=1}^{N_{j,l}} \underline{Y}_{(i,k)(j,l)}^{(m,n)} \underline{U}_j \,. \tag{10}$$

The total current of the i^{th} phase or the neutral is

$$\underline{I}_i = \sum_{k=1}^{N_i} \sum_{m=1}^{N_{i,k}} \underline{I}_{i,k}^{(m)} \,. \tag{11}$$

By inserting Eq. (10) into Eq. (11), we obtain

$$\underline{I}_i = \sum_{j=1}^{N_c} \underline{Y}_{i,j} \underline{U}_j \,, \tag{12}$$

where

$$\underline{Y}_{i,j} = \sum_{k=1}^{N_i} \sum_{m=1}^{N_{i,k}} \sum_{l=1}^{N_j} \sum_{n=1}^{N_{j,l}} \underline{Y}_{(i,k)(j,l)}^{(m,n)} \,. \tag{13}$$

From the admittance matrix with elements given by Eq. (13), we can determine the impedance matrix of a three-phase system busbars with or without the neutral busbar an the enclosure as follows

$$\underline{\boldsymbol{Z}} = \left[\underline{Z}_{i,j}\right] = \underline{\boldsymbol{Y}}^{-1} = \left[\underline{Y}_{i,j}\right]^{-1} \,. \tag{14}$$

Since each $\underline{Z}_{i,j}$ is obtained from a matrix whose elements are comprised of information related only to construction and material, its value is not affected by the busbar current. In spite of that the skin and proximity effects are taken into consideration.

If we assume all sinusoidal phase currents to be given, we can write that the neutral current $\underline{I}_N = \underline{I}_1 + \underline{I}_2 + \underline{I}_3$ and, from Eq. (12), find all voltages across phase and neutral busbars as follows:

$$\underline{U}_i = \sum_{j=1}^{N_c} \underline{Z}_{i,j} \underline{I}_j \,. \tag{15}$$

Thus, from that and Eq. (12) it is possible to determine all currents in subbars, and finally calculate, according to Eq. (2), current densities in them.

Magnetic field

Knowing the currents in each subbar – Eq. (10), the evaluation of the magnetic field can be performed. The vector magnetic potential $\underline{\boldsymbol{A}}_{i,k}^{(m)}(X)$ induced by the m^{th} subbar (Fig. 3) is given by

$$\underline{\boldsymbol{A}}_{i,k}^{(m)}(X) = \frac{\mu_0}{4\pi} \iiint_{v_{i,k}^{(m)}} \frac{\underline{\boldsymbol{J}}_{i,k}^{(m)}(Y)}{\rho_{XY}} \mathrm{d}v = \mathbf{a}_z \underline{A}_{i,k}^{(m)}(x,y,z) \,, \tag{16}$$

where $X = (x, y, z)$, $Y = (x_1, y_1, z_1)$, and $\rho_{XY} = |X - Y|$.

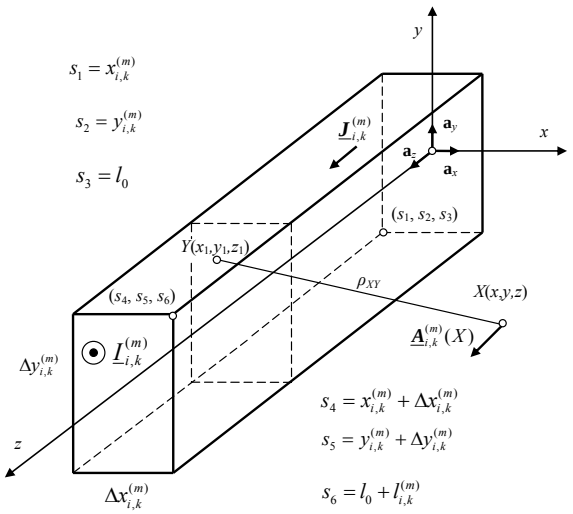

Fig. 3. The m^{th} subbar of the k^{th} bar of the i^{th} phase with the current $\underline{I}_{i,k}^{(m)}$ which generates the vector magnetic potential $\underline{\boldsymbol{A}}_{i,k}^{(m)}$ at point X

If $l_{i,k}^{(m)} >> \Delta x_{i,k}^{(m)}$ and $l_{i,k}^{(m)} >> \Delta y_{i,k}^{(m)}$ as well as $|x - x_1| >> \Delta x_{i,k}^{(m)}$ and $|y - y_1| >> \Delta y_{i,k}^{(m)}$, integral (16) can be rewritten as

$$\underline{A}_{i,k}^{(m)}(x,y,z) = \frac{\mu_0 \underline{I}_{i,k}^{(m)}}{4\pi} \int_{l_0}^{l_0 + l_{i,k}^{(m)}} \frac{\mathrm{d}z_1}{\rho_{XY}^{(m)}}, \tag{17}$$

where

$$\rho_{XY}^{(m)} = \sqrt{(x - x_{i,k}^{(m)} - \tfrac{1}{2}\Delta x_{i,k}^{(m)})^2 + (y - y_{i,k}^{(m)} - \tfrac{1}{2}\Delta y_{i,k}^{(m)})^2 + (z - z_1)^2}. \tag{18}$$

Hence, the complex magnetic field strength has two components, only, which are given by

$$\underline{H}_{x,i,k}^{(m)}(X) = -\frac{\underline{I}_{i,k}^{(m)}}{4\pi} \int_{l_0}^{l_0 + l_{i,k}^{(m)}} \frac{(y - y_{i,k}^{(m)} - \frac{1}{2}\Delta y_{i,k}^{(m)})}{(\rho_{XY}^{(m)})^3} \mathrm{d}z_1, \tag{19}$$

and

$$\underline{H}_{y,i,k}^{(m)}(X) = \frac{\underline{I}_{i,k}^{(m)}}{4\pi} \int_{l_0}^{l_0 + l_{i,k}^{(m)}} \frac{(x - x_{i,k}^{(m)} - \frac{1}{2}\Delta x_{i,k}^{(m)})}{(\rho_{XY}^{(m)})^3} \mathrm{d}z_1. \tag{19a}$$

The integrals in Eqs. (19) and (19a) are the standard integrals whose solutions are known. Let us denote

$$\Im(z,a,b) = \int \frac{b\,\mathrm{d}\xi}{[a^2 + b^2 + \xi^2]^{3/2}} = \frac{b}{a^2 + b^2} \frac{\xi}{\sqrt{a^2 + b^2 + \xi^2}} \tag{20}$$

for $\xi = z - z_1$. Thus, assuming $l_0 = 0$, the components of the magnetic field can be rewritten as

$$\underline{H}_{x,i,k}^{(m)}(X) = \frac{\underline{I}_{i,k}^{(m)}}{4\pi} \left[\Im(z, x - x_{i,k}^{(m)} - \tfrac{1}{2}\Delta x_{i,k}^{(m)}, y - y_{i,k}^{(m)} - \tfrac{1}{2}\Delta y_{i,k}^{(m)}) - \Im(l_{i,k}^{(m)} - z, x - x_{i,k}^{(m)} - \tfrac{1}{2}\Delta x_{i,k}^{(m)}, y - y_{i,k}^{(m)} - \tfrac{1}{2}\Delta y_{i,k}^{(m)}) \right], \tag{21}$$

and

$$\underline{H}_{y,i,k}^{(m)}(X) = -\frac{\underline{I}_{i,k}^{(m)}}{4\pi} \left[\Im(z, y - y_{i,k}^{(m)} - \tfrac{1}{2}\Delta y_{i,k}^{(m)}, x - x_{i,k}^{(m)} - \tfrac{1}{2}\Delta x_{i,k}^{(m)}) - \Im(l_{i,k}^{(m)} - z, y - y_{i,k}^{(m)} - \tfrac{1}{2}\Delta y_{i,k}^{(m)}, x - x_{i,k}^{(m)} - \tfrac{1}{2}\Delta x_{i,k}^{(m)}) \right]. \tag{21a}$$

The total magnetic field is given by

$$\underline{H}_x(X) = \sum_{i=1}^{N_c} \sum_{k=1}^{N_i} \sum_{m=1}^{N_{i,k}} \underline{H}_{x,i,k}^{(m)}(X), \tag{22}$$

and

$$\underline{H}_y(X) = \sum_{i=1}^{N_c} \sum_{k=1}^{N_i} \sum_{m=1}^{N_{i,k}} \underline{H}_{y,i,k}^{(m)}(X). \tag{22a}$$

In three-phase busbar systems, the magnetic field is elliptical. Its instantaneous value equals

$$\boldsymbol{H}(X,t) = \mathbf{a}_x \sqrt{2}\,\mathrm{Re}(\underline{H}_x e^{\mathrm{j}\omega t}) + \mathbf{a}_y \sqrt{2}\,\mathrm{Re}(\underline{H}_y e^{\mathrm{j}\omega t}), \tag{23}$$

and its major and minor RMS values, respectively, can be found as follows:

$$H_{\max}(X) = \max_{0 \le t \le T} \frac{|\boldsymbol{H}(X,t)|}{\sqrt{2}} = |\underline{H}_1(X)| + |\underline{H}_2(X)|, \tag{24}$$

$$H_{\min}(X) = \min_{0 \le t \le T} \frac{|\boldsymbol{H}(X,t)|}{\sqrt{2}} = \big||\underline{H}_1(X)| - |\underline{H}_2(X)|\big|, \tag{24a}$$

where

$$\underline{H}_1(X) = \frac{\underline{H}_x(X) + \mathrm{j}\,\underline{H}_y(X)}{2}, \tag{25}$$

$$\underline{H}_1(X) = \frac{\underline{H}_x^*(X) + \mathrm{j}\,\underline{H}_y^*(X)}{2}. \tag{25a}$$

Numerical examples

The first numerical example selected for this paper features a three-phase system of rectangular busbars with one neutral busbar, whose cross-section is depicted in Fig.1. According to the notations applied in this figure, the following geometry of the busbars has been selected: the dimensions of the phase rectangular busbars and the neutral busbars are a = 60 mm, $b = b_1$ = 5 mm, $d = d_1$ = 90 mm. The phase busbars and the neutral are made of copper, which has the electric conductivity of σ = 56 MS·m^{-1}. The frequency is 50 Hz. All phases have two busbars per phase − $N_1 = N_2 = N_3$ = 2, and the neutral has one busbar − N_4 = 1. The length of the busbar system is assumed to be l = 10 m. In the numerical procedure, each phase busbar is divided into $N_x^{(i,k)}$ = 30 and $N_y^{(i,k)}$ = 5, which gives 150 subbars for each busbar. Hence, all three phases and the neutral busbars have 1050 subbars in total. With the chosen division, each rectangular subbar has dimensions of 2 × 1 mm. This allows for the fact that the current density is uniform on the surface of the subbars. During the simulation, three balanced currents with busbar-rated values I_1 = 1 kA are imposed in phases as shown

$$\underline{I}_2 = \underline{I}_1 \mathrm{e}^{-\mathrm{j}120^\circ}, \quad \underline{I}_3 = \underline{I}_1 \mathrm{e}^{\mathrm{j}120^\circ}, \quad \text{and} \quad \underline{I}_N = \underline{I}_1 + \underline{I}_2 + \underline{I}_3 = 0. \tag{25}$$

As a first result, the current density comparison along x axis, practically the same along y axis at x = const, in each busbar is shown in Fig. 4.

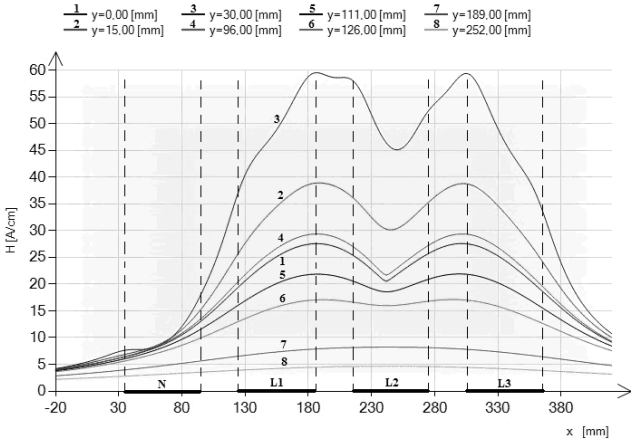

Fig. 4. Magnetic field $H_{\max}$ (RMS value) against x at different heights in the high-current three-phase busducts with two busbars per phase and one neutral bar in the case of three balanced currents (a_1 = 35 mm, b_2 = 45 mm - see Fig. 1)

The case of three unbalanced currents

$$\underline{I}_2 = 0.5\underline{I}_1 \mathrm{e}^{-\mathrm{j}120^\circ}, \quad \underline{I}_3 = \underline{I}_1 \mathrm{e}^{\mathrm{j}120^\circ}, \quad \text{and} \quad \underline{I}_N = \underline{I}_1 + \underline{I}_2 + \underline{I}_3 = 0.5\,\mathrm{e}^{\mathrm{j}60^\circ} \tag{26}$$

has been also investigated – Fig. 5.

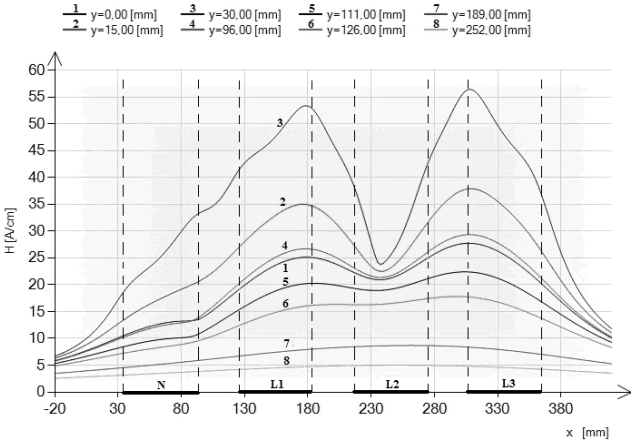

Fig. 5. Magnetic field $H_{\max}$ (RMS value) against x at different heights in the high-current three-phase busducts with two busbars per phase and one neutral bar in the case of three unbalanced currents (a_1 = 35 mm, b_2 = 45 mm - see Fig. 1)

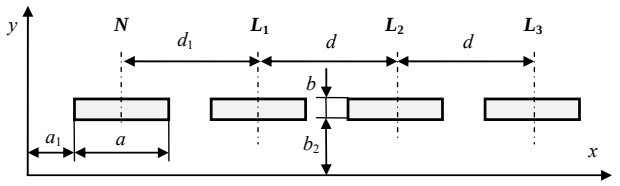

Fig. 6. Three phase high-current bus duct of rectangular cross-section with one busbar per phase and one neutral busbar

The second configuration of a three phase busbar system, the current density of which are investigated, is shown in Fig. 6. It has only one busbar per phase and neutral - $N_1 = N_2 = N_3 = N_4 = 1$. The length of the busbar system and the busbar division are as in the previous example (150 subbars for each busbar). Hence, all three phase and the neutral busbars have 600 total subbars. With the chosen division, each rectangular subbar has still dimensions of 2 × 1 mm. During the simulation, three balanced – Eq. (25) − and three unbalanced – Eq. (26) − currents with busbar-rated values I_{eff} = 1 kA are imposed in phases, and the current densities comparison along x axis, practically the same along y axis at x = const., in each busbar are shown in Fig. 7 and Fig. 8, respectively.

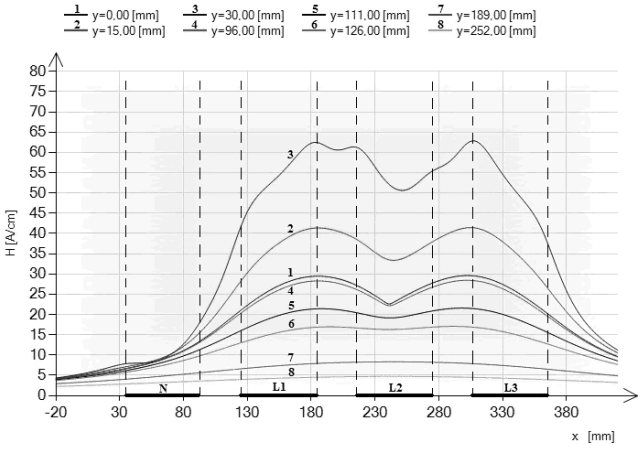

Fig. 7. Magnetic field $H_{\max}$ (RMS value) against x at different heights in the high-current three-phase busducts with one busbar per phase and one neutral bar in the case of three balanced currents (a_1 = 35 mm, b_2 = 45 mm - see Fig. 6)

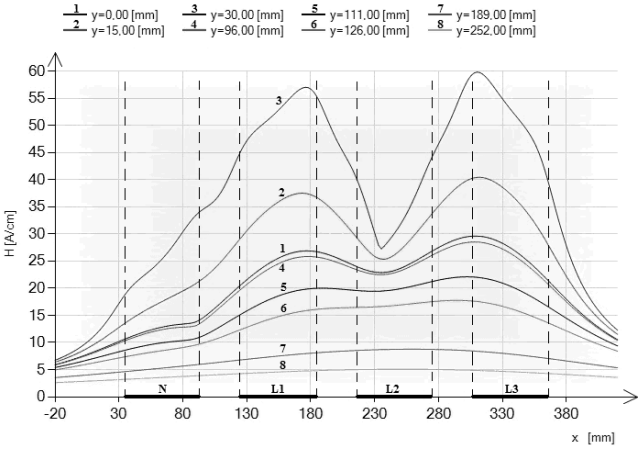

Fig. 8. Magnetic field $H_{\max}$ (RMS value) against x at different heights in the high-current three-phase busducts with one busbar per phase and one neutral bar in the case of three unbalanced currents (a_1 = 35 mm, b_2 = 45 mm - see Fig. 6)

Conclusions

A novel approach to the solution of the magnetic field distribution in the high-current bus ducts of rectangular cross-section has been presented in this paper. The proposed approach combines the Partial Element Equivalent Circuit (PEEC) method with the exact closed formulae for AC self and mutual inductances of rectangular conductors of any dimensions, which allows the precise accounting for the skin and proximity effects. Complete electromagnetic coupling between the phase busbars and the neutral busbar is taken into account as well.

Figures 4 and 5 as well as 7 and 8 show that both the skin effect and proximity effect will generally cause the magnetic field distribution differs considerably from the expected one without taking into account both effects, especially very near the busbars. Knowing the magnetic field and current distribution, the evaluation of the electrodynamic force on each busbar can be performed.

The proposed method allows us to calculate the magnetic field intensity distribution in a set of parallel rectangular busbars of any dimensions including any length. The model is strikingly simple, and from a logical stand-point can be applied in general to conductors of any cross-section, whereas many conventional methods, being much more complicated, often require a greater or lesser degree of symmetry. From the practical stand-point of the calculations involved, the model requires the solution of a rather large set of linear simultaneous equations. However, this solution is well within the range of the ability of existing computers, even those slightly overage.

REFERENCES

[1] Ducluzaux A.: *Extra losses caused in high current conductors by skin and proximity effects*. Schneider Electric "Cahier Technique" no. 83, 1983.

[2] Sarajčev P. and Goič R.: *Power loss computation in high-current generator bus ducts of rectangular cross-section*. Electris Power Components and Systems, No. 39, 2010, pp. 1469-1485.

[3] Keiko T. et al: *Calculation of magnetic fields of the bus bar*. UPEC'95, Vol. 2, 1995, pp. 554-557.

[4] Cucu M. and Popescu M.O.: *Magnetic field in encapsulated bus-bar*. U.P.B. Sci. Bull., Series C, Vol. 73, Iss. 1, 2011, pp. 129-142.

[5] Sha X. et al: *Analysis of 3-D electromagnetic field for three-phase low voltage and heavy current busbar bridge system.* Inter, J. of App. Electromagn. and Machanics, No.26, 2007, pp. 37-49.

[6] Bottausio O. et al.: *Numerical and experimental evaluation of magnetic field generated by power busbar systems.* IEE Proc.-Gener. Transm. Distrib., Vol. 143, No. 5, 1996, pp. 455-460.

[7] Piątek Z.: *Impedances of tubular high current busducts*. Polish Academy of Sciences. Warsaw 2008.

[8] Zhou J. and Lewis A.M.: *Thin-skin electromagnetic fields around a rectangular conductor bar.* J.Phus. D: Appl. Phys., No. 27, 1994, pp. 419-425.

[9] Kazimierczuk M. K.: *High-frequency magnetic components.* J Wiley & Sons, Chichester, 2009.

[10] Abdelbagi H.A.: *Skin and proximity effect in two parallel plates.* Thesis of Master of Science in Engineering, Wirght State University, 2007.

[11] Sarajčev P.: *Numerical analysis of the magnetic field of high-current busducts and GIL systems*. Energies, No.4, 2011, pp. 2196-2211.

[12] Canova A. and Giaccone L.: *Numerical and analytical modeling of busbar systems.* IEEE Trans. on Power Delivery, vol. 24, No. 3, July 2009, pp. 1568- 1577.

[13] Bourmanne P. et al.: *Skin effect and proximity effect in multiconductor systems with applied currents and voltages.* J. Appl. Phys., Vol. 69, No. 8, 1991, pp. 5035-5037.

[14] Greconici M., Madescu G. and Mot M.: *Skin effect in a free space conductor*. Facta Universitatis (NIŠ), Ser. Elec. Energ., Vol. 23, No. 2, 2010, pp. 207-215.

[15] Jafari-Shapoorabadi R., Konrad A. and Sinlair A.N.: *Comparison of three formulations for eddy-current and skin effect problems.* IEEE Trans. on Magnetics, Vol. 38, No. 2, 2002, pp. 617-620.

[16] Piątek Z. et al.: *Numerical method of computing impedances of a three-phase busbar system of rectangular cross section.* Przegląd Elektrotechniczny (Electrical Review), 2013 (to be published).

[17] Paul C. R.: *Inductance: loop and partial.* J Wiley & Sons, New Jersey, 2010.

[18] Piątek Z. and Baron B.: *Exact closed form formula for self inductance of conductor of rectangular cross section.* Progress in Electromagnetics Research M. Vol. 26, 2012, pp. 225-236.

[19] Piątek Z. et al: *Exact closed form formula for mutual inductance of conductors of rectangular cross section*. Przegląd Elektrotechniczny (Electrical Review), R. 89, No. 3a, 2013, pp. 61-64.

[20] Baron B. et al.: *Impedance of an isolated rectangular conductor*. Przegląd Elektrotechniczny (Electrical Review), 2013 (to be published).

[21] Piątek Z. et al.: *Elliptical magnetic field in high-current busducts* (in Polish). Przegląd Elektrotechniczny (Electrical Review), R. 86, No. 4, 2010, pp. 101-106.

Authors

Prof. dr hab. inż. Zygmunt Piątek, Pol. Częstochowska, Instytut Inżynierii Środowiska, e-mail: zygmunt.piatek@interia.pl

Prof. dr hab. inż. Bernard Baron, Pol. Opolska, Instytut Układów Elektromechanicznych i Elektroniki Przemysłowej, e-mail: b.baron@po.opole.pl

Dr hab. inż. Paweł Jabłoński, Pol. Częstochowska, Instytut Elektrotechniki Przemysłowej, e-mail: paweljablonski7@gmail.com

Dr inż. Tomasz Szczegielniak, Pol. Częstochowska, Instytut Inżynierii Środowiska, e-mail: szczegielniakt@interia.pl

Dr inż. Dariusz Kusiak, Pol. Częstochowska, Instytut Elektrotechniki Przemysłowej, e-mail: dariuszkusiak@wp.pl

Dr inż. Artur Pasierbek, Pol. Śląska, Instytut Elektrotechniki i Informatyki, e-mail: artur.pasierbek@polsl.pl